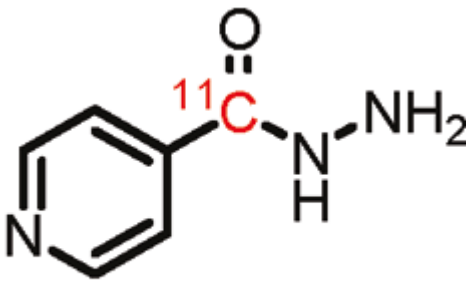


# <sup>11</sup>C-Labeled isoniazid

[<sup>11</sup>C]INH

Liang Shan, PhD<sup>1</sup>

Created: August 2, 2010; Updated: October 1, 2010.

<b>Chemical name:</b>	<sup>11</sup> C-Labeled isoniazid	
<b>Abbreviated name:</b>	[ <sup>11</sup> C]INH	
<b>Synonym:</b>	<sup>11</sup> C-Labeled isonicotinylhydrazine	
<b>Agent Category:</b>	Compounds	
<b>Target:</b>	Synthesis of mycolic acid	
<b>Target Category:</b>	Enzymes (bacteria)	
<b>Method of detection:</b>	Positron emission tomography (PET)	
<b>Source of signal / contrast:</b>	<sup>11</sup> C	
<b>Activation:</b>	No	
<b>Studies:</b>	<ul style="list-style-type: none"><li><i>In vitro</i></li><li>Non-human primates</li></ul>	

Structure of [<sup>11</sup>C]INH by Liu et al (1). Click on the [PubChem](#) for additional information about INH.

## Background

[PubMed]

Isoniazid, also known as isonicotinylhydrazine (INH), is a first-line drug used in the prevention and treatment of tuberculosis (TB) (1, 2). INH is a prodrug that is activated by

<sup>1</sup> National Center for Biotechnology Information, NLM, NIH; Email: micad@ncbi.nlm.nih.gov.

<sup>✉</sup> Corresponding author.

NLM Citation: Shan L. <sup>11</sup>C-Labeled isoniazid. 2010 Aug 2 [Updated 2010 Oct 1]. In: Molecular Imaging and Contrast Agent Database (MICAD) [Internet]. Bethesda (MD): National Center for Biotechnology Information (US); 2004-2013.

the catalase-peroxidase enzyme KatG of the mycobacteria. The activation process leads to the formation of the isonicotinic acyl-NADH complex. Subsequent binding of the complex with the enoyl-acyl carrier protein reductase InhA results in the inhibition of mycolic acid synthesis, which is essential for the wall of mycobacteria (3). INH is bactericidal to rapidly dividing mycobacteria but is bacteriostatic to slow-growing mycobacteria. INH labeled with  $^{11}\text{C}$  ( $[^{11}\text{C}]\text{INH}$ ) has been generated by Liu et al. for *in vivo* and real-time analysis of the INH pharmacokinetics (PK) and biodistribution with positron emission tomography (PET) (1). The half-life of  $^{11}\text{C}$  is 20.4 min, allowing for a ~60 min window to observe the PK.

The PK and biodistribution of a novel drug are traditionally determined with blood and tissue sampling and/or autoradiography. Despite high workload and huge investment in drug development, only 8% of the drugs entering clinical trials today reach the market, as estimated by the U.S. [Food and Drug Administration](#). One main reason for this attrition is insufficient exploration of the *in vivo* drug–target interaction (1). Traditional methods are inadequate to answer questions such as whether a drug reaches the target, how the drug interacts with its targets, and how the drug modifies the diseases. Because of the high resolution and sensitivity of newly developed imaging techniques, investigators have become increasingly interested in addressing these issues (4, 5). In the case of PET imaging, most small molecules can now be efficiently labeled with  $^{11}\text{C}$  or with  $^{18}\text{F}$  at  $>37$  GBq/ $\mu\text{mol}$  (1 Ci/ $\mu\text{mol}$ ), and they can be detected with PET in the nanomolar to picomolar concentration range (6–8). Consequently, a sufficient signal for imaging can be obtained even though the total amount of a radiotracer administered systemically is extremely low (known as microdosing, typically  $<1$   $\mu\text{g}$  for humans). Microdosing is particularly valuable for evaluating tissue exposure in the early phase of drug development when the full-range toxicology is not yet available (9, 10). Increasing evidence has demonstrated the efficiency of PET imaging in obtaining quantitative information on drug PK and distribution in various tissues including brain; confirming drug binding with targets and elucidating the relationship between occupancy and target expression/function *in vivo*; assessing drug passage across the blood–brain barrier (BBB) and ensuring sufficient exposure to brain for central nervous system drugs; and dissecting the modifying effects of drugs on diseases (4, 6, 7).

The current treatment regime for drug-sensitive TB involves the use of rifampicin (RIF), INH, pyrazinamide (PZA), and ethambutol or streptomycin for two months, followed by four months of continued dosing with INH and RIF (11, 12). This regime is primarily based on PK studies in serum and on efficacy of treatment. The efficacy of each drug for different types of TB such as brain TB and the drug distribution in each compartment of an organ are not well understood. To provide direct insights into these drugs, Liu et al. labeled INH, RIF, and PZA with  $^{11}\text{C}$  and used PET to investigate their PK and biodistribution in baboons (1). Liu et al. found that the organ distribution and BBB penetration of each drug differed greatly. The ability of  $[^{11}\text{C}]\text{INH}$  to penetrate the BBB was lower than that of PZA but higher than that of RIF (PZA  $>$  INH  $>$  RIF). The INH concentrations in the lungs and brain were ten times higher than the INH minimum inhibitory concentration (MIC) value against TB, supporting the use of INH for treating

TB infections in the lungs and brain. This chapter summarizes the data obtained by Liu et al. regarding [<sup>11</sup>C]INH. The data obtained with regard to [<sup>11</sup>C]RIF and [<sup>11</sup>C]PZA are described in the MICAD chapters on [<sup>11</sup>C]RIF and [<sup>11</sup>C]PZA, respectively.

### Related Resource Links:

- [Challenge and Opportunity on the Critical Path to New Medical Products, FDA](#)
- [Isoniazid compounds in PubChem Substance](#)
- [Clinical trials for diagnosis and treatment of tuberculosis in ClinicalTrials.gov](#)
- [MICAD chapters on \[<sup>11</sup>C\]RIF and \[<sup>11</sup>C\]PZA](#)

## Synthesis

[\[PubMed\]](#)

Liu et al. synthesized [<sup>11</sup>C]INH in three steps, starting with [<sup>11</sup>C]HCN. The first step involved treatment of iodopyridine with [<sup>11</sup>C]HCN and catalysis with tetrakis(triphenylphosphine)palladium to form [<sup>11</sup>C]cyanopyridine. This step gave 90% radiochemical yield. Subsequent hydrazine hydrolysis of the cyanide was accomplished in two steps, which involved a nucleophilic attack by hydrazine and subsequent hydrolysis of the imine by water.

The final product was generated with an average 45%–50% decay-corrected yield (calculated from [<sup>11</sup>C]HCN) with a total synthesis time of 50 min. Isonicotinamide was the only major byproduct, with <15% of the total yield being isonicotinamide. The radiolabeled product was >99% radiochemically pure with a specific activity of 5.18–5.92 GBq/μmol (140–165 mCi/μmol).

## *In Vitro* Studies: Testing in Cells and Tissues

[\[PubMed\]](#)

Liu et al. determined the plasma protein binding (% of free fraction in plasma) of [<sup>11</sup>C]INH after incubation with baboon plasma for 10 min at room temperature. The plasma protein binding was 27.32%, which is similar to literature values reported elsewhere (1). The lipophilicity of [<sup>11</sup>C]INH was not measured.

## Animal Studies

### Rodents

[\[PubMed\]](#)

No references are currently available.

### Other Non-Primate Mammals

[\[PubMed\]](#)

No references are currently available.

## Non-Human Primates

[PubMed]

Liu et al. used PET imaging to study the biodistribution of [ $^{11}\text{C}$ ]INH in healthy baboons ( $n = 4$ ) (1). The INH concentrations in the brain and other organs were estimated on the basis of the weight of the baboon, a standard daily dose (5 mg/kg for a human adult), and the assumption that the positron signal derives primarily from the intact drug. Studies showed that the penetrating ability of [ $^{11}\text{C}$ ]INH through the BBB was weaker than that of PZA but better than that of RIF. The INH concentration in the brain tissue was higher than in the cerebrospinal fluid. The concentration in the whole brain was 0.00299% injected dose per cubic centimeter (ID/cc) (2.54  $\mu\text{g}/\text{ml}$ ) at 30 min, 0.00248% ID/cc (2.11  $\mu\text{g}/\text{ml}$ ) at 60 min, and 0.00206% ID/cc (1.75  $\mu\text{g}/\text{ml}$ ) at 90 min after injection, which was ten times higher than its MIC against TB, suggesting that INH is a suitable drug for the treatment of brain TB infection as previously recommended.

The detailed data about the [ $^{11}\text{C}$ ]INH distribution in other organs were presented in table 3 in the paper published by Liu et al (1). In general, [ $^{11}\text{C}$ ]INH and/or its metabolites rapidly penetrated the heart, lungs, liver, and kidneys. In most organs, the INH concentration exceeded that observed in plasma over the 90-min period. The calculated concentration was more than ten times higher than its MIC, supporting the use of INH for treating TB infections. However, Liu et al. noticed in the literature differences between the INH concentrations in organs among different species, which were explained by the interspecies variation and radionuclide difference (1).

## Human Studies

[PubMed]

No references are currently available.

## References

1. Liu L., Xu Y., Shea C., Fowler J.S., Hooker J.M., Tonge P.J. *Radiosynthesis and bioimaging of the tuberculosis chemotherapeutics isoniazid, rifampicin and pyrazinamide in baboons*. J Med Chem. 2010;53(7):2882–91. PubMed PMID: 20205479.
2. Hall R.G., Leff R.D., Gumbo T. *Treatment of active pulmonary tuberculosis in adults: current standards and recent advances. Insights from the Society of Infectious Diseases Pharmacists*. Pharmacotherapy. 2009;29(12):1468–81. PubMed PMID: 19947806.
3. Lu X.Y., You Q.D., Chen Y.D. *Recent progress in the identification and development of InhA direct inhibitors of Mycobacterium tuberculosis*. Mini Rev Med Chem. 2010;10(3):181–92. PubMed PMID: 20408801.

4. Fox G.B., Chin C.L., Luo F., Day M., Cox B.F. *Translational neuroimaging of the CNS: novel pathways to drug development*. Mol Interv. 2009;9(6):302–13. PubMed PMID: 20048136.
5. Komoda F., Suzuki A., Yanagisawa K., Inoue T. *Bibliometric study of radiation application on microdose useful for new drug development*. Ann Nucl Med. 2009;23(10):829–41. PubMed PMID: 19862482.
6. Hammond L.A., Denis L., Salman U., Jerabek P., Thomas C.R. Jr, Kuhn J.G. *Positron emission tomography (PET): expanding the horizons of oncology drug development*. Invest New Drugs. 2003;21(3):309–40. PubMed PMID: 14578681.
7. Lancelot, S. and L. Zimmer, *Small-animal positron emission tomography as a tool for neuropharmacology*. Trends Pharmacol Sci, 2010
8. Lee C.M., Farde L. *Using positron emission tomography to facilitate CNS drug development*. Trends Pharmacol Sci. 2006;27(6):310–6. PubMed PMID: 16678917.
9. Bauer M., Wagner C.C., Langer O. *Microdosing studies in humans: the role of positron emission tomography*. Drugs R D. 2008;9(2):73–81. PubMed PMID: 18298126.
10. Wagner C.C., Muller M., Lappin G., Langer O. *Positron emission tomography for use in microdosing studies*. Curr Opin Drug Discov Devel. 2008;11(1):104–10. PubMed PMID: 18175273.
11. Tomioka H. *Current status of some antituberculosis drugs and the development of new antituberculous agents with special reference to their in vitro and in vivo antimicrobial activities*. Curr Pharm Des. 2006;12(31):4047–70. PubMed PMID: 17100611.
12. Aristoff P.A., Garcia G.A., Kirchhoff P.D., Hollis Showalter H.D. *Rifamycins--obstacles and opportunities*. Tuberculosis (Edinb). 2010;90(2):94–118. PubMed PMID: 20236863.